

Data-Driven Controlled Invariant Sets for Gaussian Process State Space Models

Paul Griffioen^{a,*}, Bingzhuo Zhong^{b,*}, Murat Arcak^a, Majid Zamani^c,
Marco Caccamo^d

^a*Department of Electrical Engineering and Computer Sciences, University of California, Berkeley, Berkeley, CA, USA 94720*

^b*Thrust of Artificial Intelligence, Information Hub, Hong Kong University of Science and Technology (Guangzhou), Guangzhou, Guangdong, China 511453*

^c*Department of Computer Science, University of Colorado Boulder, Boulder, CO, USA 80309*

^d*School of Engineering and Design, Technical University of Munich, Garching, Germany 85748*

Abstract

We compute probabilistic controlled invariant sets for nonlinear systems using Gaussian process state space models, which are data-driven models that account for unmodeled and unknown nonlinear dynamics. We investigate the relationship between robust and probabilistic invariance, leveraging this relationship to design state-feedback controllers that maximize the probability of the system staying within the probabilistic controlled invariant set. We propose a semi-definite-programming-based optimization scheme for designing the state-feedback controllers subject to input constraints. The effectiveness of our results are demonstrated and validated on a quadrotor, both in simulation and on a physical platform.

Key words: Gaussian processes, probabilistic controlled invariance, safety, data-based control

1 Introduction

Gaussian Process State Space Models (GPSSMs) are powerful dynamical models that are increasingly used to account for the nonlinearities and unknown dynamics of physical systems [10–12, 27, 29, 30]. In contrast to parametric models like recurrent neural networks, GPSSMs are inherently regularized by a prior model, mitigating the tendency to overfit. Furthermore, GPSSMs quantify

uncertainty and modeling errors as a distribution over functions, ensuring that the model is not overconfident in regions of the state space where data is scarce [8, 24]. GPSSMs are commonly employed in safety critical applications [32–34], in which system failures, such as collisions, may result in catastrophic consequences. For these applications, it is crucial to design controllers that prevent the system from reaching unsafe regions of the state space.

* P. Griffioen and B. Zhong are authors who contributed equally.

**This work was supported in part by the Air Force Office of Scientific Research under Grant FA9550-21-1-0288 and the National Science Foundation under Grants CNS-2111688, CNS-2145184, and CNS-2039062. Marco Caccamo was supported by an Alexander von Humboldt Professorship endowed by the German Federal Ministry of Education and Research.

Email addresses: griffioen@berkeley.edu (Paul Griffioen), bingzhuo.zhong@hkust-gz.edu.cn (Bingzhuo Zhong), arcak@berkeley.edu (Murat Arcak), majid.zamani@colorado.edu (Majid Zamani), mcaccamo@tum.de (Marco Caccamo).

To ensure safety, abstraction-based approaches have been studied in [1, 9, 16, 36]. Instead of considering continuous state and input sets, these approaches discretize the state and input sets of the original system to construct finite abstractions. As a result, the number of discrete states and inputs grows exponentially with the dimensions of the state and input sets, respectively, limiting their applicability to high-dimensional systems. In contrast, invariant sets [3] can be computed without an abstraction to ensure the safety of the system under the effects of uncertainties. In particular, robust invariant sets (RIS) [2, 5, 6] are used to describe a region of the state space in which the state trajectory is guaranteed

to remain under unknown but bounded disturbances. Similarly, probabilistic invariant sets (PIS) [17, 18, 22] have been proposed to describe a set in which the state trajectory remains at all times with a certain probability. The relationship between RIS and PIS for linear systems is examined in [15].

Other results, such as [28, 31], provide robust invariance guarantees via barrier functions, but they do not treat the uncertainty as probabilistic. Instead, uncertainty is treated as a fixed function for which the Gaussian Process (GP) regression model provides a prediction with pointwise error bounds. The result in [14] extends the probabilistic invariance results in [15, 17, 18] to nonlinear systems that take the form of GPSSMs but does not synthesize controllers to maximize the probability of keeping the systems within the PIS. Data-driven control synthesis for uncertain control systems is addressed in [7, 21, 37]. However, the results only apply to linear systems with unknown-but-bounded disturbances instead of nonlinear systems containing stochastic uncertainty.

In this paper, we set forth a semi-definite-programming (SDP)-based methodology to jointly compute probabilistic controlled invariant (PCI) sets along with state feedback controllers for nonlinear systems modeled by GPSSMs. Here, the probabilistic uncertainty is attributed to unknown components of the model as well as noise. Accordingly, the synthesized controller guarantees that the state trajectory of the system will stay within the associated PCI set with a certain probability at all time steps.

The contributions of this paper include the following. We present methods for verifying PCI sets, investigating the relationship between robust invariance and probabilistic invariance. We then propose an optimization problem for jointly computing PCI sets and their associated state feedback controllers for GPSSMs. Lastly, we demonstrate the applicability of our results on a physical experimental platform (quadrotor) in addition to Monte Carlo simulation.

The remainder of this paper is structured as follows. In Section 2, we introduce the system model, GPSSMs, and the main problem we seek to address. Section 3 investigates the relationship between robust invariance and probabilistic invariance, providing a more general formulation and proof details that are not present in [14, 15]. Then in Section 4 we discuss how to both verify and design safety controllers for probabilistic controlled invariant sets. To demonstrate the effectiveness of our results, we apply the joint controller and PCI set computation to two case studies in Section 5. We give the conclusions in Section 6.

Notation We let \oplus represent the Minkowski sum and $\|\cdot\|_2$ be the Euclidean norm. Given a random variable s , we let $\mathbb{E}[s]$ and $\text{Cov}[s]$ represent its expected value and

covariance, respectively. We let $\text{Diag}(s_1, \dots, s_{\bar{n}})$ represent a diagonal matrix with elements $s_1, \dots, s_{\bar{n}}$ on the diagonal. We also let $\text{BlkDiag}(S_1, \dots, S_{\bar{n}})$ represent a block diagonal matrix with matrices $S_1, \dots, S_{\bar{n}}$ on each block.

2 Gaussian Process State Space Models

2.1 System Model

We consider a discrete time system model with a continuous-valued state, where uncertainty in the model is captured by n independent GPs, given by

$$x_{k+1} = g(x_k, u_k) + w_k, \quad (1)$$

where $x_k \in \mathbb{R}^n$ represents the system state at time step k and $u_k \in U \subseteq \mathbb{R}^m$ is the control input vector. The input constraints are given by

$$U \triangleq \{u \in \mathbb{R}^m \mid \zeta_i^T u \leq 1, i = 1, \dots, n_u\}, \quad (2)$$

where n_u denotes the number of constraints and ζ_i represents the i^{th} input constraint. The term $w_k \sim \mathcal{N}(0, Q)$ is independent and identically distributed (i.i.d.) GP noise with $Q \triangleq \text{Diag}(\sigma_1^2, \dots, \sigma_n^2)$. The term $g(x_k, u_k)$ is defined as

$$g(x_k, u_k) \triangleq \begin{bmatrix} g_1(x_k, u_k) \\ \vdots \\ g_n(x_k, u_k) \end{bmatrix}, \quad (3)$$

$$g_i(x_k, u_k) \sim \mathcal{GP}(m_i(\hat{x}_k), k_i(\hat{x}_k, \hat{x}'_k)), \hat{x}_k \triangleq \begin{bmatrix} x_k \\ u_k \end{bmatrix}, \quad (4)$$

where $g_i(x_k, u_k)$ is a GP specified by its mean function $m_i(\hat{x}_k): \mathbb{R}^{n+m} \rightarrow \mathbb{R}$ and covariance function $k_i(\hat{x}_k, \hat{x}'_k): \mathbb{R}^{n+m} \times \mathbb{R}^{n+m} \rightarrow \mathbb{R}$. These are given by

$$m_i(\hat{x}_k) \triangleq A_i x_k + B_i u_k, \quad (5)$$

$k_i(\hat{x}_k, \hat{x}'_k) \triangleq \mathbb{E}[(g_i(\hat{x}_k) - m_i(\hat{x}_k))(g_i(\hat{x}'_k) - m_i(\hat{x}'_k))]$, (6) where A_i and B_i denote the i^{th} rows of A and B , respectively. We assume that $A \triangleq [A_1^T \dots A_n^T]^T$, $B \triangleq [B_1^T \dots B_n^T]^T$, $\{g_1, \dots, g_n\}$, and Q are unknown. A GP is a distribution over functions, assigning a joint Gaussian distribution to any finite subset of the state and control input space [23]. The covariance function of a GP is also called the kernel function of the process, which determines the class of functions over which the distribution is defined.

We assume that N measurements of the state are taken, either through recorded trajectory data or simply by sampling the state transition function at various

points in the state and control input space. This training data set, composed of N data pairs, is given by $\mathcal{D} \triangleq \{\{\bar{x}_j, \bar{u}_j\}, \bar{x}_j^+\}_{j=1}^N$, where

$$\bar{x}_j^+ = g(\bar{x}_j, \bar{u}_j) + w_j, \quad w_j \sim \mathcal{N}(0, Q), \quad (7)$$

with w_j being the observation noise. The training data can be used to determine the values of the hyperparameters for the mean function and the covariance function by optimizing the marginal likelihood [23]. Given input training data $\{\bar{x}_j, \bar{u}_j\}_{j=1}^N$ and output training data $\{\bar{x}_j^+\}_{j=1}^N$, $g(x_k, u_k)$ conditioned on x_k, u_k , and \mathcal{D} follows a Gaussian distribution, given by

$$g(x_k, u_k) | \{x_k, u_k, \mathcal{D}\} \sim \mathcal{N}(\mu(\hat{x}_k), \Sigma(\hat{x}_k)), \quad (8)$$

$$\mu(\hat{x}_k) \triangleq \begin{bmatrix} m_1(\hat{x}_k) + \bar{k}_1(\hat{x}_k)^T (K_1 + \sigma_1^2 I_N)^{-1} (y_1 - \bar{y}_1) \\ \vdots \\ m_n(\hat{x}_k) + \bar{k}_n(\hat{x}_k)^T (K_n + \sigma_n^2 I_N)^{-1} (y_n - \bar{y}_n) \end{bmatrix},$$

$$\Sigma(\hat{x}_k) \triangleq \begin{bmatrix} \xi_1(\hat{x}_k) & \cdots & 0 \\ \vdots & \ddots & \vdots \\ 0 & \cdots & \xi_n(\hat{x}_k) \end{bmatrix},$$

$$\xi_i(\hat{x}_k) \triangleq k_i(\hat{x}_k, \hat{x}_k) - \bar{k}_i(\hat{x}_k)^T (K_i + \sigma_i^2 I_N)^{-1} \bar{k}_i(\hat{x}_k),$$

$$K_i \triangleq \begin{bmatrix} k_i(\hat{x}_1, \hat{x}_1) & \cdots & k_i(\hat{x}_1, \hat{x}_N) \\ \vdots & \ddots & \vdots \\ k_i(\hat{x}_N, \hat{x}_1) & \cdots & k_i(\hat{x}_N, \hat{x}_N) \end{bmatrix}, \quad \hat{x}_j \triangleq \begin{bmatrix} \bar{x}_j \\ \bar{u}_j \end{bmatrix},$$

$$\bar{k}_i(\hat{x}_k) \triangleq \begin{bmatrix} k_i(\hat{x}_1, \hat{x}_k) \\ \vdots \\ k_i(\hat{x}_N, \hat{x}_k) \end{bmatrix}, \quad y_i \triangleq \begin{bmatrix} \bar{x}_1^+(i) \\ \vdots \\ \bar{x}_N^+(i) \end{bmatrix}, \quad \bar{y}_i \triangleq \begin{bmatrix} m_i(\hat{x}_1) \\ \vdots \\ m_i(\hat{x}_N) \end{bmatrix},$$

where $\bar{x}_j^+(i)$ denotes the i^{th} dimension of \bar{x}_j^+ .

2.2 Problem Formulation

Let the safety constraints be given by

$$X \triangleq \{x \in \mathbb{R}^n | \beta_i^T x \leq 1, i = 1, \dots, n_x\}, \quad (9)$$

where n_x denotes the number of constraints and β_i represents the i^{th} state constraint. Given this set of safety constraints, we would like to design a state feedback controller $u_k = Lx_k$ to maximize the probability of safety. This can be described more formally as follows.

Problem 1 *Given the system in (1), design a controller $u_k = Lx_k$ to maximize $\Pr(x_k \in X | x_0 \in X) \forall k$ such that $u_k \in U$ when $x_k \in X$.*

3 Robust and Probabilistic Invariance

In order to solve Problem 1, we first introduce a few tools that will be used in the design of the controller. These tools include robust positive invariance, confidence regions, and probabilistic positive invariance which will ultimately be used to derive a linear matrix inequality (LMI) constraint in the verification and design of the controller that solves Problem 1.

3.1 Robust Positive Invariance

Before introducing robust positive invariance, we first define an ellipsoid in Definition 1, introduce one of the properties of ellipsoids in Corollary 1, and then present the system model to which robust positive invariance is referenced.

Definition 1 *An ellipsoid is given by*

$$\mathcal{E}(\bar{\mu}, \bar{\Sigma}) \triangleq \bar{\mu} \oplus \left\{ \bar{\Sigma}^{\frac{1}{2}} s \mid \|s\|_2 \leq 1 \right\}, \quad (10)$$

where $\bar{\mu}$ is the center and $\bar{\Sigma} = \bar{\Sigma}^T \succeq 0$ is the shape matrix.

Corollary 1 ([25]) *Let $\bar{\Sigma}_1 = \bar{\Sigma}_1^T \succeq 0$ and $\bar{\Sigma}_2 = \bar{\Sigma}_2^T \succeq 0$. Then*

$$\mathcal{E}(0, \bar{\Sigma}_1 + \bar{\Sigma}_2) \subseteq \mathcal{E}(0, \bar{\Sigma}_1) \oplus \mathcal{E}(0, \bar{\Sigma}_2). \quad (11)$$

PROOF. Follows from Definition 1 as well as Theorem 8.1, Definition 2.1, and Proposition 2.2 in [25]. ■

Consider a system of the form

$$z_{k+1} = \mathcal{A}z_k + \mathcal{B}d_k + \mathcal{C}v_k, \quad (12)$$

where $d_k \in \mathcal{E}(\mu_d, \Sigma_d) \subset \mathbb{R}^{n_d}$ and $v_k \in \mathcal{E}(\mu_v, \Sigma_v) \subset \mathbb{R}^{n_v}$ are unknown but bounded disturbances and $z_k \in \mathbb{R}^{n_z}$.

Definition 2 ([2]) *The set Z is a robustly positively invariant set for (12) if*

$$z_0 \in Z \implies z_k \in Z \forall k \geq 0. \quad (13)$$

Theorem 1 presents a sufficient condition in the form of an LMI for robust positive invariance.

Theorem 1 *Given a system described by (12), the set $\mathcal{E}(c, \mathcal{P}^{-1})$ remains robustly positively invariant for (12)*

provided there exists an $\alpha \geq 0$ such that

$$\begin{bmatrix} \Phi_{11} & \Phi_{12} & \Phi_{13} & \Phi_{14} \\ \Phi_{12}^T & \Phi_{22} & \Phi_{23} & \Phi_{24} \\ \Phi_{13}^T & \Phi_{23}^T & \Phi_{33} & \Phi_{34} \\ \Phi_{14}^T & \Phi_{24}^T & \Phi_{34}^T & \Phi_{44} \end{bmatrix} \succeq 0, \quad (14)$$

$$\begin{aligned} \Phi_{11} &\triangleq (1-\alpha)\mathcal{P} - \mathcal{A}^T\mathcal{P}\mathcal{A}, \\ \Phi_{12} &\triangleq -\mathcal{A}^T\mathcal{P}\mathcal{B}, \\ \Phi_{13} &\triangleq -\mathcal{A}^T\mathcal{P}\mathcal{C}, \\ \Phi_{14} &\triangleq (\alpha-1)\mathcal{P}c + \mathcal{A}^T\mathcal{P}c, \\ \Phi_{22} &\triangleq \frac{1}{2}\alpha\Sigma_d^{-1} - \mathcal{B}^T\mathcal{P}\mathcal{B}, \\ \Phi_{23} &\triangleq -\mathcal{B}^T\mathcal{P}\mathcal{C}, \\ \Phi_{24} &\triangleq \mathcal{B}^T\mathcal{P}c - \frac{1}{2}\alpha\Sigma_d^{-1}\mu_d, \\ \Phi_{33} &\triangleq \frac{1}{2}\alpha\Sigma_v^{-1} - \mathcal{C}^T\mathcal{P}\mathcal{C}, \\ \Phi_{34} &\triangleq \mathcal{C}^T\mathcal{P}c - \frac{1}{2}\alpha\Sigma_v^{-1}\mu_v, \\ \Phi_{44} &\triangleq (1-\alpha)c^T\mathcal{P}c + \frac{1}{2}\alpha\mu_d^T\Sigma_d^{-1}\mu_d + \frac{1}{2}\alpha\mu_v^T\Sigma_v^{-1}\mu_v. \end{aligned}$$

PROOF. From the lossless S-procedure [4], (14) is equivalent to

$$\begin{aligned} &\begin{bmatrix} z_k \\ d_k \\ v_k \end{bmatrix}^T \begin{bmatrix} -\mathcal{P} & 0 & 0 \\ 0 & \frac{1}{2}\Sigma_d^{-1} & 0 \\ 0 & 0 & \frac{1}{2}\Sigma_v^{-1} \end{bmatrix} \begin{bmatrix} z_k \\ d_k \\ v_k \end{bmatrix} + 2 \begin{bmatrix} \mathcal{P}c \\ -\frac{1}{2}\Sigma_d^{-1}\mu_d \\ -\frac{1}{2}\Sigma_v^{-1}\mu_v \end{bmatrix}^T \begin{bmatrix} z_k \\ d_k \\ v_k \end{bmatrix} \\ &\quad - c^T\mathcal{P}c + \frac{1}{2}\mu_d^T\Sigma_d^{-1}\mu_d + \frac{1}{2}\mu_v^T\Sigma_v^{-1}\mu_v \leq 0 \implies \\ &\begin{bmatrix} z_k \\ d_k \\ v_k \end{bmatrix}^T \begin{bmatrix} \mathcal{A}^T\mathcal{P}\mathcal{A} - \mathcal{P} & \mathcal{A}^T\mathcal{P}\mathcal{B} & \mathcal{A}^T\mathcal{P}\mathcal{C} \\ \mathcal{B}^T\mathcal{P}\mathcal{A} & \mathcal{B}^T\mathcal{P}\mathcal{B} & \mathcal{B}^T\mathcal{P}\mathcal{C} \\ \mathcal{C}^T\mathcal{P}\mathcal{A} & \mathcal{C}^T\mathcal{P}\mathcal{B} & \mathcal{C}^T\mathcal{P}\mathcal{C} \end{bmatrix} \begin{bmatrix} z_k \\ d_k \\ v_k \end{bmatrix} \\ &\quad + 2 \begin{bmatrix} c^T\mathcal{P}(I-\mathcal{A}) & -c^T\mathcal{P}\mathcal{B} & -c^T\mathcal{P}\mathcal{C} \end{bmatrix} \begin{bmatrix} z_k \\ d_k \\ v_k \end{bmatrix} - c^T\mathcal{P}c \leq 0. \end{aligned}$$

This in turn is equivalent to

$$\begin{aligned} &-(z_k - c)^T\mathcal{P}(z_k - c) + \frac{1}{2}(d_k - \mu_d)^T\Sigma_d^{-1}(d_k - \mu_d) \\ &\quad + \frac{1}{2}(v_k - \mu_v)^T\Sigma_v^{-1}(v_k - \mu_v) \leq 0 \implies \quad (15) \\ &(\mathcal{A}z_k + \mathcal{B}d_k + \mathcal{C}v_k - c)^T\mathcal{P}(\mathcal{A}z_k + \mathcal{B}d_k + \mathcal{C}v_k - c) \\ &\quad - (z_k - c)^T\mathcal{P}(z_k - c) \leq 0. \end{aligned}$$

Note that

$$\begin{aligned} &\left\{ \begin{array}{l} (z_k - c)^T\mathcal{P}(z_k - c) \geq 1 \\ (d_k - \mu_d)^T\Sigma_d^{-1}(d_k - \mu_d) \leq 1 \\ (v_k - \mu_v)^T\Sigma_v^{-1}(v_k - \mu_v) \leq 1 \end{array} \right\} \implies \quad (16) \\ &-(z_k - c)^T\mathcal{P}(z_k - c) + \frac{1}{2}(d_k - \mu_d)^T\Sigma_d^{-1}(d_k - \mu_d) \\ &\quad + \frac{1}{2}(v_k - \mu_v)^T\Sigma_v^{-1}(v_k - \mu_v) \leq 0. \end{aligned}$$

Combining the implications in (15) and (16) yields that

$$\begin{aligned} &\left\{ \begin{array}{l} (z_k - c)^T\mathcal{P}(z_k - c) \geq 1 \\ (d_k - \mu_d)^T\Sigma_d^{-1}(d_k - \mu_d) \leq 1 \\ (v_k - \mu_v)^T\Sigma_v^{-1}(v_k - \mu_v) \leq 1 \end{array} \right\} \implies \\ &\quad (z_{k+1} - c)^T\mathcal{P}(z_{k+1} - c) \leq (z_k - c)^T\mathcal{P}(z_k - c), \end{aligned}$$

which is in turn equivalent to

$$\begin{aligned} &(z_k - c)^T\mathcal{P}(z_k - c) \geq 1 \implies \\ &\quad (z_{k+1} - c)^T\mathcal{P}(z_{k+1} - c) \leq (z_k - c)^T\mathcal{P}(z_k - c) \quad (17) \\ &\quad \forall d_k \in \mathcal{E}(\mu_d, \Sigma_d), \forall v_k \in \mathcal{E}(\mu_v, \Sigma_v). \end{aligned}$$

In [2], it is shown that $\mathcal{E}(c, \mathcal{P}^{-1})$ is a robustly positively invariant set for (12) if and only if (17) holds. This concludes the proof, as we have shown (14) implies that $\mathcal{E}(c, \mathcal{P}^{-1})$ is a robustly positively invariant set for (12). ■

3.2 Confidence Regions

Before introducing probabilistic positive invariance, we first define confidence regions in Definition 3 and one of their properties in Corollary 2. These will serve as necessary prerequisites for analyzing the relationship between robust and probabilistic invariance.

Definition 3 ([15]) *The set S is a confidence region of probability level p for a random variable s , denoted by $C_p(s)$, if*

$$\Pr(s \in S) \geq p. \quad (18)$$

Corollary 2 characterizes a confidence region that holds for an arbitrary distribution.

Corollary 2 *Let $\bar{\mu} = \mathbb{E}[s]$ and $\bar{\Sigma} = \text{Cov}[s]$, where $s \in \mathbb{R}^{n_s}$ is a random variable. Then for any $p \in [0, 1]$,*

$$\mathcal{E}\left(\bar{\mu}, \frac{n_s}{1-p}\bar{\Sigma}\right) \text{ is a } C_p(s). \quad (19)$$

PROOF. Follows from Definition 1 and the multidimensional Chebyshev inequality. ■

3.3 Probabilistic Positive Invariance

Consider a system of the form

$$z_{k+1} = \mathcal{A}_k z_k + \mathcal{B}_k d_k + \mathcal{C}_k v_k(z_k), \quad (20)$$

where $z_k \in \mathbb{R}^{n_z}$, $d_k \in D_k \subset \mathbb{R}^{n_d}$ is an unknown but bounded term, and $v_k(z_k) \in \mathbb{R}^{n_v}$ is a random variable.

Definition 4 ([15]) *The set Z is a probabilistic positively invariant set of probability level p for (20) if*

$$z_0 \in Z \implies \Pr(z_k \in Z) \geq p \quad \forall k \geq 0. \quad (21)$$

To establish a relationship between robust and probabilistic invariance, we introduce the deterministic system

$$\bar{z}_{k+1} = \mathcal{A}_k \bar{z}_k + \mathcal{B}_k d_k + \mathcal{C}_k \bar{v}_k(\bar{z}_k), \quad (22)$$

which is identical to (20) except that $\bar{v}_k(\bar{z}_k) \in V_k \subset \mathbb{R}^{n_v}$ is an unknown but bounded term.

Lemma 1 *Consider the systems in (20) and (22), letting Z be a robustly positively invariant set for (22). Suppose there exists a sequence of sets \bar{Z}_k , $k \geq 0$, such that $\bar{Z}_0 \subseteq Z$,*

$$\bar{Z}_{k+1} \subseteq \mathcal{A}_k \bar{Z}_k \oplus \mathcal{B}_k D_k \oplus \mathcal{C}_k V_k \quad \forall k \geq 0, \quad (23)$$

and \bar{Z}_k is a $C_p(z_k)$ for (20) $\forall k \geq 0$. Then Z is also a probabilistic positively invariant set of probability level p for (20).

PROOF. Since Z is a robustly positively invariant set for (22),

$$\mathcal{A}_k Z \oplus \mathcal{B}_k D_k \oplus \mathcal{C}_k V_k \subseteq Z \quad \forall k \geq 0. \quad (24)$$

Combining (23) and (24) yields

$$\bar{Z}_k \subseteq Z \implies \bar{Z}_{k+1} \subseteq Z \quad \forall k \geq 0. \quad (25)$$

Since $\bar{Z}_0 \subseteq Z$, it follows from (25) that $\bar{Z}_k \subseteq Z \quad \forall k \geq 0$. Since, further, \bar{Z}_k is a $C_p(z_k)$ for (20) $\forall k \geq 0$, Z is a $C_p(z_k)$ for (20) $\forall k \geq 0$. ■

Theorem 2 leverages the result in Lemma 1 to establish the relationship between robust and probabilistic positive invariance.

Theorem 2 *Consider the systems in (20) and (22), letting $V_k = \mathcal{E}(0, \frac{n_z}{1-p} \bar{\Sigma}_k^v)$, where $\bar{\Sigma}_k^v \succeq \text{Cov}[v_k(z_k)|z_k] \quad \forall k \geq 0$. If $\mathbb{E}[v_k(z_k)|z_k] = 0 \quad \forall k \geq 0$ and if Z is a robustly positively invariant set for (22) (with respect to $V_k \quad \forall k \geq 0$), then Z is also a probabilistic positively invariant set of probability level p for (20).*

PROOF. Let $\mu_k^z \triangleq \mathbb{E}[z_k]$ and $\Sigma_k^z \triangleq \text{Cov}[z_k]$. In what follows, we will show that (23) is satisfied with $\bar{Z}_k = \mathcal{E}(\mu_k^z, \frac{n_z}{1-p} \Sigma_k^z)$. Given the system dynamics in (20), note that

$$\begin{aligned} \mu_{k+1}^z &\in \mathcal{A}_k \mu_k^z \oplus \mathcal{B}_k D_k \oplus \mathcal{C}_k \mathbb{E}[v_k(z_k)] \\ &= \mathcal{A}_k \mu_k^z \oplus \mathcal{B}_k D_k \oplus \mathcal{C}_k \mathbb{E}[\mathbb{E}[v_k(z_k)|z_k]] \\ &= \mathcal{A}_k \mu_k^z \oplus \mathcal{B}_k D_k, \end{aligned} \quad (26)$$

$$\begin{aligned} \mathbb{E}[z_{k+1}|z_k] &= \mathcal{A}_k z_k + \mathcal{B}_k d_k + \mathcal{C}_k \mathbb{E}[v_k(z_k)|z_k] \\ &= \mathcal{A}_k z_k + \mathcal{B}_k d_k, \end{aligned} \quad (27)$$

$$\text{Cov}[z_{k+1}|z_k] = \mathcal{C}_k \text{Cov}[v_k(z_k)|z_k] \mathcal{C}_k^T, \quad (28)$$

where the first equality in (26) follows from the law of total expectation and the second equalities in (26) and (27) follow from the fact that $\mathbb{E}[v_k(z_k)|z_k] = 0$. Also note that

$$\begin{aligned} \Sigma_{k+1}^z &= \text{Cov}[\mathbb{E}[z_{k+1}|z_k]] + \mathbb{E}[\text{Cov}[z_{k+1}|z_k]] \\ &= \text{Cov}[\mathcal{A}_k z_k + \mathcal{B}_k d_k] + \mathbb{E}[\mathcal{C}_k \text{Cov}[v_k(z_k)|z_k] \mathcal{C}_k^T] \\ &= \mathcal{A}_k \Sigma_k^z \mathcal{A}_k^T + \mathcal{C}_k \mathbb{E}[\text{Cov}[v_k(z_k)|z_k]] \mathcal{C}_k^T \\ &\preceq \mathcal{A}_k \Sigma_k^z \mathcal{A}_k^T + \mathcal{C}_k \bar{\Sigma}_k^v \mathcal{C}_k^T, \end{aligned} \quad (29)$$

where the first equality follows from the law of total covariance, the second equality follows from (27) and (28), the third equality follows from the fact that d_k is an unknown but bounded term, and the inequality follows from the fact that $\text{Cov}[v_k(z_k)|z_k] \preceq \bar{\Sigma}_k^v$. Then $\forall k \geq 0$,

$$\begin{aligned} \mathcal{E}\left(\mu_{k+1}^z, \frac{n_z}{1-p} \Sigma_{k+1}^z\right) &= \mu_{k+1}^z \oplus \mathcal{E}\left(0, \frac{n_z}{1-p} \Sigma_{k+1}^z\right) \\ &\subseteq \mathcal{A}_k \mu_k^z \oplus \mathcal{B}_k D_k \oplus \mathcal{E}\left(0, \frac{n_z}{1-p} (\mathcal{A}_k \Sigma_k^z \mathcal{A}_k^T + \mathcal{C}_k \bar{\Sigma}_k^v \mathcal{C}_k^T)\right) \\ &\subseteq \mathcal{A}_k \mu_k^z \oplus \mathcal{B}_k D_k \oplus \mathcal{E}\left(0, \frac{n_z}{1-p} \mathcal{A}_k \Sigma_k^z \mathcal{A}_k^T\right) \\ &\quad \oplus \mathcal{E}\left(0, \frac{n_z}{1-p} \mathcal{C}_k \bar{\Sigma}_k^v \mathcal{C}_k^T\right) \\ &= \mathcal{A}_k \mathcal{E}\left(\mu_k^z, \frac{n_z}{1-p} \Sigma_k^z\right) \oplus \mathcal{B}_k D_k \oplus \mathcal{C}_k \mathcal{E}\left(0, \frac{n_z}{1-p} \bar{\Sigma}_k^v\right), \end{aligned}$$

where the first and last equalities follow from Definition 1, the first inequality follows from (26) and (29), and the second inequality follows from Corollary 1. The claim then follows from Lemma 1 since:

- $\mathcal{E}(\mu_k^z, \frac{n_z}{1-p} \Sigma_k^z)$ is a $C_p(z_k)$ for (20) $\forall k \geq 0$ according to Corollary 2;
- $\mathcal{E}(\mu_0^z, \frac{n_z}{1-p} \Sigma_0^z) \subseteq Z$ because $\mu_0^z \in Z$ and $\Sigma_0^z = 0$ since $z_0 \in Z$ according to Definition 4. ■

Theorem 3 combines all the previous results regarding the relationship between robust and probabilistic invariance in preparation for the application to GPSSMs.

Theorem 3 Consider a system as in (20) with $\mathcal{A}_k = \mathcal{A}$, $\mathcal{B}_k = \mathcal{B}$, $\mathcal{C}_k = \mathcal{C}$, $D_k = \mathcal{E}(\mu_d, \Sigma_d)$, $\mathbb{E}[v_k(z_k)|z_k] = 0$, and $\bar{\Sigma}_v \succeq \text{Cov}[v_k(z_k)|z_k]$ for some $\bar{\Sigma}_v \succeq 0 \forall k \geq 0$. If $\exists \alpha \geq 0$, $c \in \mathbb{R}^{n_z}$, $\mathcal{P} \succ 0$ such that (14) is satisfied when $\mu_v = 0$ and when $\frac{n_z}{1-p} \bar{\Sigma}_v$ is substituted for Σ_v , then $\mathcal{E}(c, \mathcal{P}^{-1})$ is a probabilistic positively invariant set of probability level p for (20).

PROOF. Follows from Theorems 1 and 2. \blacksquare

4 Probabilistic Controlled Invariant Sets

Returning to the system dynamics in (1), note that they can be written equivalently as

$$x_{k+1} = Ax_k + Bu_k + \hat{\mu}(\hat{x}_k) + \mathcal{I}\bar{w}_k(\hat{x}_k), \quad (30)$$

where $\hat{\mu}(\hat{x}_k) \triangleq \mu(\hat{x}_k) - [m_1(\hat{x}_k) \cdots m_n(\hat{x}_k)]^T$, $\mathcal{I} \triangleq [I_n \ I_n]$, $\bar{w}_k(\hat{x}_k) \triangleq [\bar{g}(x_k, u_k)^T \ w_k^T]^T$, and

$$\bar{g}(x_k, u_k) | \{x_k, u_k, \mathcal{D}\} \sim \mathcal{N}(0, \Sigma(\hat{x}_k)). \quad (31)$$

We now present methods for both the verification and design of controllers that will ensure probabilistic invariance for the system in (30). In doing so, we make the following assumption regarding the system in (1) (and consequently the system in (30)):

Assumption 1 The GPs g and \bar{g} in (1) and (30) have stationary covariance functions.

Note that Assumption 1 is not a very restrictive assumption since most covariance functions are stationary, including constant, exponential, squared exponential, γ -exponential, rational quadratic, Mátérn, and many others [23, Table 4.1].

4.1 Controller Verification

Lemma 2 shows how the mean of the GPSSM is bounded, which is used in the proof of Theorem 4 to provide a sufficient condition for probabilistic invariance.

Lemma 2 ([14]) For the system in (30),

$$\hat{\mu}(\hat{x}_k) \in \mathcal{E}(0, \phi I_n) \forall k \geq 0, \quad (32)$$

where $\phi \triangleq \sum_{i=1}^n (k_i^T (K_i + \sigma_i^2 I_N)^{-1} (y_i - \bar{y}_i))^2$ and $\hat{k}_i \triangleq [k_i(\hat{x}_k, \hat{x}_k) \cdots k_i(\hat{x}_k, \hat{x}_k)]^T \in \mathbb{R}^N$ which is a constant.

Theorem 4 leverages the result in Lemma 2 to provide a sufficient condition for probabilistic invariance.

Theorem 4 Consider a system in (30) with control $u_k = Lx_k$. Suppose $\exists \alpha \geq 0$, $P \succ 0$ such that

$$\begin{bmatrix} (1-\alpha)P - A_{bl}^T P A_{bl} & -A_{bl}^T P & -A_{bl}^T P \mathcal{I} \\ -P A_{bl} & \frac{\alpha}{2\phi} I_n - P & -P \mathcal{I} \\ -\mathcal{I}^T P A_{bl} & -\mathcal{I}^T P & \frac{\alpha(1-p)}{2n} \bar{Q}^{-1} - \mathcal{I}^T P \mathcal{I} \end{bmatrix} \succeq 0, \quad (33)$$

where $A_{bl} \triangleq A + BL$, $\bar{Q} \triangleq \text{BlkDiag}(\hat{\Sigma}, Q)$, and $\hat{\Sigma} \triangleq \text{Diag}(k_1(\hat{x}_k, \hat{x}_k), \dots, k_n(\hat{x}_k, \hat{x}_k))$, which is a constant. Then $\mathcal{E}(0, P^{-1})$ is a probabilistic positively invariant set of probability level p .

PROOF. Follows from Lemma 2, Theorem 3, and the fact that $\hat{\Sigma} \succeq \Sigma(\hat{x}_k) \forall \hat{x}_k \in \mathbb{R}^{n+m}$. \blacksquare

4.2 Controller Design

We now formally define probabilistic controlled invariance in Definition 5 and present how to design controllers associated with probabilistic controlled invariant sets in Theorems 5 and 6.

Definition 5 The set $\mathcal{X} \in \mathbb{R}^n$ is a probabilistic controlled invariant (PCI) set of probability level p for (30) if there exists a controller $u_k = Lx_k$ such that \mathcal{X} is a probabilistic positively invariant set of probability level p for (30).

Theorem 5 Consider a system in (30) with control $u_k = Lx_k$. Then $\mathcal{E}(0, P^{-1})$ is a PCI set of probability level p for (30) if $\exists \alpha \geq 0$, $P \succ 0$ such that (33) is satisfied and

$$\beta_i^T P^{-1} \beta_i \leq 1, \quad i = 1, \dots, n_x, \quad (34)$$

$$\zeta_j^T L P^{-1} L^T \zeta_j \leq 1, \quad j = 1, \dots, n_u. \quad (35)$$

PROOF. According to [26, Lemma 4.1], (34) is equivalent to $\mathcal{E}(0, P^{-1}) \subseteq X$, ensuring that the PCI set of probability level p lies within the state constraints. Similarly, according to [26, Section 4.2], (35) is equivalent to $L\mathcal{E}(0, P^{-1}) \subseteq U$, ensuring that $u_k \in U$ when $u_k = Lx_k$ and $x_k \in \mathcal{E}(0, P^{-1})$. The result then follows from Theorem 4. \blacksquare

Lemma 3 and Theorem 6 present an optimization problem as a more direct method for how to design the controller L to ensure probabilistic invariance.

Lemma 3 For the system in (30), if for some $\eta \in [0, 1]$,

$$x_k \in \mathcal{E}(0, P^{-1}) \implies (Ax_k + Bu_k)^T P (Ax_k + Bu_k) \leq \eta, \quad (36)$$

$$HP^{-1}H^T \succeq \frac{1}{(1-\sqrt{\eta})^2}I_n, \quad H^TH = \Theta(p), \quad (37)$$

$$\Theta(p) \triangleq \begin{bmatrix} I_n & \mathcal{I} \end{bmatrix} \begin{bmatrix} 2\phi I_n & 0 \\ 0 & \frac{2n}{1-p}\bar{Q} \end{bmatrix} \begin{bmatrix} I_n \\ \mathcal{I}^T \end{bmatrix},$$

then $\mathcal{E}(0, P^{-1})$ is a robustly positively invariant set for (30) when $\bar{w}_k(\hat{x}_k) \in \mathcal{E}(0, \frac{n}{1-p}\bar{Q}) \forall k \geq 0$.

PROOF. Let $\psi_k \triangleq Ax_k + Bu_k$ and $\varphi_k \triangleq \hat{\mu}(\hat{x}_k) + \mathcal{I}\bar{w}_k(\hat{x}_k)$, implying that $x_{k+1} = \psi_k + \varphi_k$. From (36), we know that $\psi_k \in \mathcal{E}(0, \eta P^{-1}) \forall k \geq 0$. According to Lemma 2, (32) holds. Consequently,

$$\left\{ \begin{array}{l} \hat{\mu}(\hat{x}_k) \in \mathcal{E}(0, \phi I_n) \forall k \geq 0 \\ \bar{w}_k(\hat{x}_k) \in \mathcal{E}(0, \frac{n}{1-p}\bar{Q}) \forall k \geq 0 \end{array} \right\} \implies \varphi_k \in \mathcal{E}(0, \Theta(p)) \forall k \geq 0.$$

We want to show that $x_{k+1} \in \mathcal{E}(0, P^{-1})$, which holds if

$$\mathcal{E}(0, \eta P^{-1}) \oplus \mathcal{E}(0, \Theta(p)) \subseteq \mathcal{E}(0, P^{-1}). \quad (38)$$

Applying a change of coordinates with $\bar{\psi}_k \triangleq H\psi_k$, $\bar{\varphi}_k \triangleq H\varphi_k$, and $\bar{P} \triangleq H^{-1T}PH^{-1}$ yields

$$\begin{aligned} \mathcal{E}(0, \eta P^{-1}) &= \{\psi_k | \bar{\psi}_k^T \bar{P} \bar{\psi}_k \leq \eta\}, \\ \mathcal{E}(0, \Theta(p)) &= \{\varphi_k | \bar{\varphi}_k^T \bar{\varphi}_k \leq 1\}, \\ \mathcal{E}(0, P^{-1}) &= \{x_{k+1} | (\bar{\psi}_k + \bar{\varphi}_k)^T \bar{P} (\bar{\psi}_k + \bar{\varphi}_k) \leq 1\}. \end{aligned}$$

Consequently, the minimum distance between the boundaries of $\mathcal{E}(0, \eta P^{-1})$ and $\mathcal{E}(0, P^{-1})$ is given by

$$\sqrt{\lambda_{\min}} - \sqrt{\eta \lambda_{\min}},$$

where λ_{\min} is the minimum eigenvalue of \bar{P}^{-1} . To ensure that (38) holds, we need to ensure that this minimum distance is greater than the radius of $\mathcal{E}(0, \Theta(p))$, which is 1. This is equivalent to ensuring that

$$\lambda_{\min} \geq \frac{1}{(1-\sqrt{\eta})^2},$$

which can be enforced by ensuring $\bar{P}^{-1} \succeq \frac{1}{(1-\sqrt{\eta})^2}I_n$. ■

Theorem 6 For the system in (30), if a controller is

designed so that $L = MP$ according to

$$\begin{aligned} &\arg \max_{p, \eta \in [0,1], P \succ 0, M} p \\ &s.t. \begin{bmatrix} P^{-1} & AP^{-1} + BM \\ P^{-1}A + M^TB^T & \eta P^{-1} \end{bmatrix} \succeq 0, \\ &HP^{-1}H^T \succeq \frac{1}{(1-\sqrt{\eta})^2}I_n, \quad H^TH = \Theta(p), \quad (39) \\ &\beta_j^T P^{-1} \beta_j \leq 1, \quad j = 1, \dots, n_x, \\ &\begin{bmatrix} P^{-1} & M^T \zeta_i \\ \zeta_i^T M & 1 \end{bmatrix} \succeq 0, \quad i = 1, \dots, n_u, \end{aligned}$$

then $\mathcal{E}(0, P^{-1})$ is a PCI set of probability level p for (30).

PROOF. According to [26, 35], the last constraint in (39) is equivalent to $MP\mathcal{E}(0, P^{-1}) \subseteq U$, ensuring that $u_k \in U$ when $u_k = MPx_k$ and $x_k \in \mathcal{E}(0, P^{-1})$. As shown in the proof of Theorem 5, the second to last constraint ensures that $\mathcal{E}(0, P^{-1}) \subseteq X$. According to [35], the first constraint is equivalent to

$$\begin{aligned} (P^{-1}A^T + M^TB^T)P(AP^{-1} + BM) &\preceq \eta P^{-1} \iff \\ P^{-1}(A + BMP)^T P(A + BMP)P^{-1} &\preceq \eta P^{-1} \iff \\ (A + BMP)^T P(A + BMP) &\preceq \eta P \iff \\ \begin{bmatrix} \eta P - (A + BMP)^T P(A + BMP) & 0 \\ 0 & \eta - \eta \end{bmatrix} &\succeq 0. \quad (40) \end{aligned}$$

By using the S-procedure [4], (40) is equivalent to

$$x_k^T P x_k \leq 1 \implies x_k^T (A + BMP)^T P (A + BMP) x_k \leq \eta$$

when $\eta \geq 0$, which in turn is equivalent to

$$x_k \in \mathcal{E}(0, P^{-1}) \implies (Ax_k + Bu_k)^T P (Ax_k + Bu_k) \leq \eta$$

when $u_k = MPx_k$. The result then follows from Lemma 3 and Theorem 2. ■

Note that the optimization problem in (39) is a semidefinite program for any fixed η and p [4]. Consequently, p can be maximized by applying bisection over p for a set of samples $\eta \in [0, 1]$. This procedure is described in detail in Algorithm 1.

Remark 1 Note that the optimization problem in line 5 of Algorithm 1 can be solved in parallel for different samples of η . Additionally, the objective function of this optimization problem maximizes the size of the PCI set $\mathcal{E}(0, P^{-1})$ for any given probability level p since the size of the set $\mathcal{E}(0, P^{-1})$ is proportional to $\log \det P^{-1}$ [4].

Algorithm 1 Optimization Problem Implementation

```

1: Initialize  $p$  and precision  $\delta$  for the bisection over  $p$ 
2:  $p_{\text{low}} = 0, p_{\text{up}} = 1$ 
3: while  $p_{\text{up}} - p_{\text{low}} > \delta$ 
4:   for Samples  $\eta \in [0, 1]$ 
5:     Given  $p$  and  $\eta$ , solve

       
$$\arg \max_{P>0, M} \log \det P^{-1}$$


       s.t. constraints in (39) are satisfied

6:   end for
7:   if Feasible for any sample  $\eta$ 
8:      $p_{\text{low}} = p$ 
9:   else
10:     $p_{\text{up}} = p$ 
11:   end if
12:    $p = (p_{\text{up}} + p_{\text{low}})/2$ 
13: end while

```

5 Case Studies

To show the effectiveness of our results, we first test them on a high fidelity **SIMULINK** model for a quadrotor and demonstrate the probabilistic guarantee through Monte Carlo analysis. Next we present physical experiments on a quadrotor platform. We trained a GPSSM using data collected from this platform, synthesized the PCI set, designed the safety controller based on the PCI set, and applied the controller to the physical quadrotor.

We consider controlling a quadrotor moving in a 2-dimensional plane (x - y plane), as shown in Figure 1, and

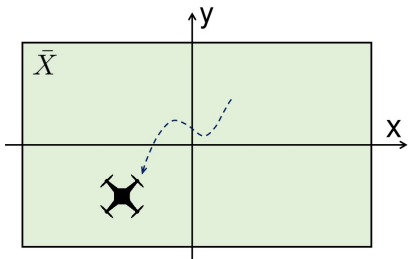


Fig. 1. A quadrotor moving on an x - y plane.

model the quadrotor dynamics as a GPSSM according to (1) with states and inputs described according to [13]. The system states and control inputs are given by $x \triangleq [x_x \ v_x \ x_y \ v_y]^T$ and $u \triangleq [u_x \ u_y]^T$, where x_i, v_i , and u_i are the position, velocity, and acceleration of the quadrotor on the i^{th} axis, respectively, with $i \in \{x, y\}$.

5.1 High Fidelity **SIMULINK** Model

First, we use a high fidelity **SIMULINK** model as shown in Figure 2 to validate the probabilistic guarantee proposed in this paper via Monte Carlo analysis. We consider state

constraints $x_x, x_y \in [-5, 5]$ m and $v_x, v_y \in [-7, 7]$ m/s, and input constraints $u_x, u_y \in [-5, 5]$ m/s².

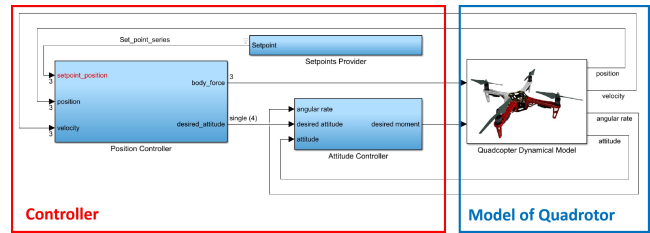


Fig. 2. High fidelity **SIMULINK** for the quadrotor.

To synthesize a PCI set for this model, we simulate the model to collect a single state-input trajectory with $N = 550$. We train the GPSSM with a squared exponential covariance function given by

$$k_i(\hat{x}_k, \hat{x}'_k) = \sigma_i e^{(\hat{x}_k - \hat{x}'_k)^T \bar{L}_i^{-2} (\hat{x}_k - \hat{x}'_k)}, \quad i \in \{1, 2, 3, 4\},$$

by using the function `fitrgp` in **MATLAB**. After this process, the trained hyperparameters are given by

$$A = \begin{bmatrix} 0.9999 & 0.1009 & -0.0001 & -0.0005 \\ -0.0018 & 1.0160 & -0.0025 & -0.0086 \\ 0 & 0.0008 & 0.9999 & 0.0996 \\ -0.0014 & 0.0149 & -0.0024 & 0.9926 \end{bmatrix},$$

$$B = \begin{bmatrix} 0.0028 & 0.0603 & -0.0017 & -0.0309 \\ -0.0017 & -0.0291 & 0.0028 & 0.0619 \end{bmatrix}^T,$$

$Q = 10^{-4} \text{Diag}(2.6429, 2.5738, 2.3335, 2.5739)$, $\sigma_1 = 1.3343 \times 10^{-5}$, $\bar{L}_1 = 9.6392 \times 10^3 I_6$, $\sigma_2 = 1.2362 \times 10^{-5}$, $\bar{L}_2 = 2.2333 \times 10^3 I_6$, $\sigma_3 = 1.2539 \times 10^{-5}$, $\bar{L}_3 = 9.6410 \times 10^3 I_6$, $\sigma_4 = 1.1428 \times 10^{-5}$, and $\bar{L}_4 = 5.0345 \times 10^3 I_6$. With this model, we obtain a PCI set $\mathcal{E}(0, P^{-1})$ with $\eta = 0.9251$, probability level $p = 99.9765\%$ and controller $u_k = Lx_k$ according to Theorem 6 using **Mosek** [20] and **YALMIP** [19], where

$$P = \begin{bmatrix} 0.0679 & 0.0671 & 0.0028 & 0.0056 \\ 0.0671 & 0.1802 & 0.0236 & 0.0330 \\ 0.0028 & 0.0236 & 0.0601 & 0.0466 \\ 0.0056 & 0.0330 & 0.0466 & 0.1130 \end{bmatrix},$$

$$L = \begin{bmatrix} -0.6162 & -1.9897 & -0.3997 & -0.8999 \\ 0.0297 & -0.8025 & -0.9550 & -1.5374 \end{bmatrix}.$$

For the simulation, we randomly select 10^6 initial states within the PCI set and simulate the **SIMULINK** model

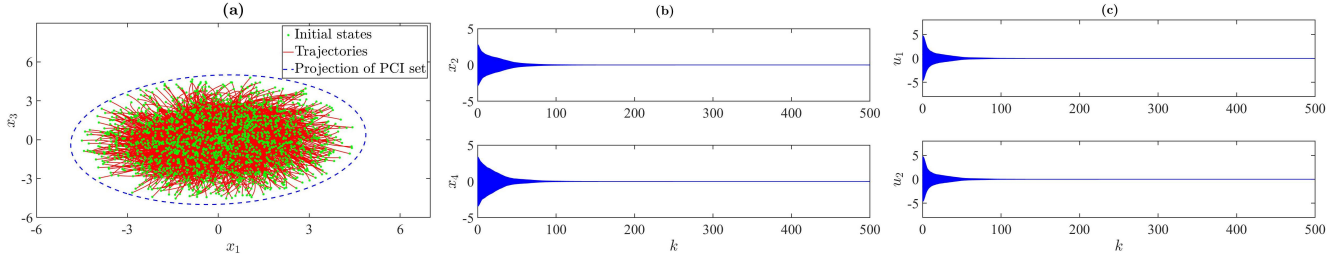


Fig. 3. Simulation results for the high fidelity SIMULINK model of the quadrotor case study. Figure (a) denotes the projection of the PCI set and some of the state trajectories of the quadrotor onto the x_1 - x_3 plane. Figure (b) demonstrates a few sequences of the velocity of the quadrotor. Figure (c) illustrates sequences of the control inputs of the quadrotor.

from each initial state for a time horizon of $T = 500$. We apply the controller $u_k = Lx_k$ associated with the PCI set to control the system among all simulations.

The simulation results are summarized in Table 1, which show that the probabilistic safety guarantees associated with the PCI set are respected. In addition, Figure 3 depicts some of the state trajectories, sequences of velocities on different axes, and control input sequences of these simulations.

$\min_{k \in [0, 500]} \Pr(x_k \in \mathcal{E}(0, P^{-1}))$	100%
$\min_{k \in [0, 500]} \Pr(u_k \in U x_k \in \mathcal{E}(0, P^{-1}))$	100%
$\Pr(x_k \in X \forall k \in [0, 500])$	100%
$\Pr(x_k \in \mathcal{E}(0, P^{-1}) \forall k \in [0, 500])$	99.99%

Table 1

Results of Monte Carlo analysis over the high fidelity SIMULINK model of the quadrotor using the controller $u_k = Lx_k$ associated with the PCI set.

5.2 Experimental Physical Testbed

To show the practicality of our design, we applied it to the physical testbed, which includes a physical quadrotor (Figure 4, left) and a test field (Figure 4, right). The test field is equipped with a motion capture system for recording the position and velocity of the quadrotor and a ground control station (GCS) for running the controller and sending the desired accelerations (i.e., the control input) to the quadrotor at runtime.



Fig. 4. Left: Physical quadrotor for the experiment. Right: Test field equipped with a motion capture system and a ground control station.

According to the setting of the physical quadrotor and the spatial restrictions of the physical test field, we consider state constraints $x_x, x_y \in [-2.5, 2.5]$ m and $v_x, v_y \in [-7, 7]$ m/s, and input constraints $u_x, u_y \in [-7, 7]$ m/s². To synthesize a PCI set for the physical quadrotor, we collect a single state-input trajectory from the quadrotor and construct a data set containing $N = 436$ data points. Based on this data set, we train the GPSSM with a squared exponential covariance function given by

$$k_i(\hat{x}_k, \hat{x}'_k) = \sigma_i e^{(\hat{x}_k - \hat{x}'_k)^T \bar{L}_i^{-2} (\hat{x}_k - \hat{x}'_k)}, \quad i \in \{1, 2, 3, 4\},$$

by using the function `fitrgp` in MATLAB. After this procedure, the trained hyperparameters are given by

$$A = \begin{bmatrix} 1.0002 & 0.1009 & -0.0001 & -0.0002 \\ -0.0023 & 0.9919 & -0.0001 & 0.0013 \\ -0.0005 & 0.0003 & 1.0001 & 0.1011 \\ -0.0039 & 0.0025 & 0.0001 & 0.9901 \end{bmatrix},$$

$$B = \begin{bmatrix} 0.0046 & 0.0720 & -0.0018 & -0.0112 \\ -0.0005 & -0.0062 & 0.0041 & 0.0844 \end{bmatrix}^T,$$

$Q = 10^{-3} \text{Diag}(0.0233, 0.1210, 0.0815, 0.1679)$, $\sigma_1 = 0.0014$, $\bar{L}_1 = 8.2882 \times 10^4 I_6$, $\sigma_2 = 0.0034$, $\bar{L}_2 = 491.0781 I_6$, $\sigma_3 = 7.7636 \times 10^{-6}$, $\bar{L}_3 = 3.3397 \times 10^7 I_6$, $\sigma_4 = 0.0063$, and $\bar{L}_4 = 644.1183 I_6$. By following the same synthesis procedure for the high fidelity model, we obtain a PCI set $\mathcal{E}(0, P^{-1})$ with $\eta = 0.8230$, probability level $p = 97.36\%$, and its associated controller $u_k = Lx_k$, where

$$P = \begin{bmatrix} 0.2790 & 0.1231 & -0.0078 & -0.0028 \\ 0.1231 & 0.1286 & 0.0103 & 0.0027 \\ -0.0078 & 0.0103 & 0.2577 & 0.0995 \\ -0.0028 & 0.0027 & 0.0995 & 0.1028 \end{bmatrix},$$

$$L = \begin{bmatrix} -2.6987 & -2.4831 & -0.1247 & -0.1870 \\ -0.2101 & -0.4243 & -2.7680 & -2.1569 \end{bmatrix}.$$

In Figure 5, we plot the quadrotor’s trajectory over 50 s (i.e., $T = 500$) as it follows a series of set points that go outside the PCI set. In Figures 5 and 6 we depict the position sequence and the sequences of velocity and control inputs of the quadrotor, respectively. As can be seen in the figures, the desired safety and input constraints are respected while the state trajectory of the quadrotor stays within the obtained PCI set. A video for the experiment can be found online: <https://youtu.be/mEuuRIm57j4>.

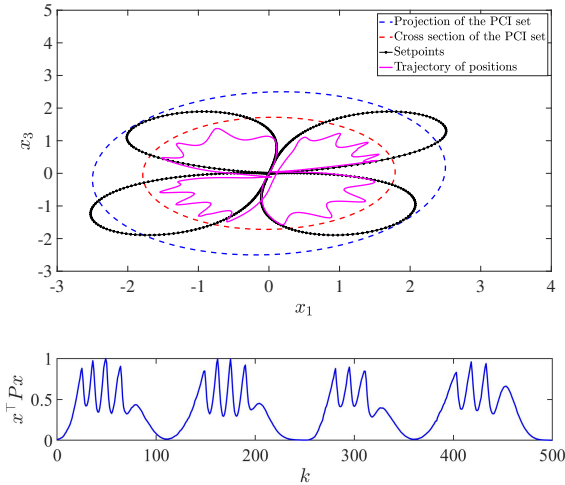


Fig. 5. Top: Evolution of the quadrotor’s positions in the real-world experiment. Bottom: Values of $x_k^T P x_k$ along the trajectory of the quadrotor.

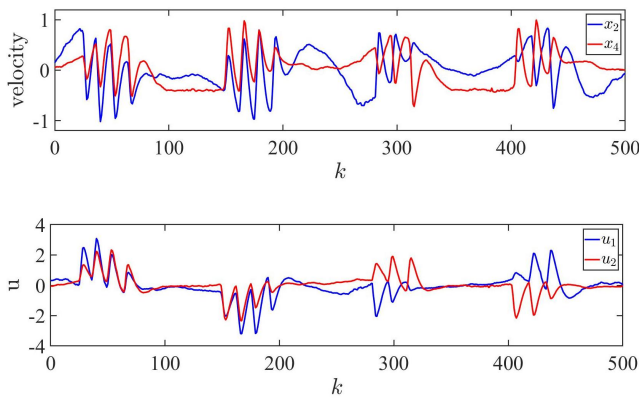


Fig. 6. Sequences of the quadrotor’s velocity and control inputs in the real-world experiment.

6 Conclusion

This paper has set forth a method for computing PCI sets and designing associated state-feedback controllers for GPSSMs. These controllers provide safety guarantees

for nonlinear systems with unmodeled and unknown dynamics. We propose an optimization scheme for computing the PCI set. Our results are illustrated on a quadrotor in both high-fidelity simulations and a physical experiment. One research direction is designing controllers according to an optimization problem that both provides safety guarantees while also maximizing performance. Another research direction is leveraging reachability analysis over GPSSMs to enlarge the size of the PCI sets.

References

- [1] Alessandro Abate, Maria Prandini, John Lygeros, and Shankar Sastry. Probabilistic Reachability and Safety for Controlled Discrete Time Stochastic Hybrid Systems. *Automatica*, 44(11):2724–2734, 2008.
- [2] Angelo Alessandri, Marco Baglietto, and Giorgio Battistelli. On Estimation Error Bounds for Receding-Horizon Filters Using Quadratic Boundedness. *IEEE Transactions on Automatic Control*, 49(8):1350–1355, 2004.
- [3] Franco Blanchini. Set Invariance in Control. *Automatica*, 35(11):1747–1767, 1999.
- [4] Stephen Boyd, Laurent El Ghaoui, Eric Feron, and Venkataramanan Balakrishnan. *Linear Matrix Inequalities in System and Control Theory*. SIAM, 1994.
- [5] Mark L Brockman and Martin Corless. Quadratic Boundedness of Nonlinear Dynamical Systems. In *Proceedings of 1995 34th IEEE Conference on Decision and Control*, volume 1, pages 504–509. IEEE, 1995.
- [6] Mark L Brockman and Martin Corless. Quadratic Boundedness of Nominally Linear Systems. *International Journal of Control*, 71(6):1105–1117, 1998.
- [7] Claus Danielson, Avishai Weiss, Karl Berntorp, and Stefano Di Cairano. Path Planning Using Positive Invariant Sets. In *2016 IEEE 55th Conference on Decision and Control (CDC)*, pages 5986–5991. IEEE, 2016.
- [8] Marc Peter Deisenroth, Dieter Fox, and Carl Edward Rasmussen. Gaussian Processes for Data-Efficient Learning in Robotics and Control. *IEEE Transactions on Pattern Analysis and Machine Intelligence*, 37(2):408–423, 2013.
- [9] Jerry Ding, Maryam Kamgarpour, Sean Summers, Alessandro Abate, John Lygeros, and Claire Tomlin. A Stochastic Games Framework for Verification and Control of Discrete Time Stochastic Hybrid Systems. *Automatica*, 49(9):2665–2674, 2013.
- [10] Stefanos Eleftheriadis, Tom Nicholson, Marc Deisenroth, and James Hensman. Identification of Gaussian Process State Space Models. *Advances in Neural Information Processing Systems*, 30, 2017.
- [11] Roger Frigola, Yutian Chen, and Carl Edward Rasmussen. Variational Gaussian Process State-Space Models. *Advances in Neural Information Processing Systems*, 27, 2014.
- [12] Roger Frigola, Fredrik Lindsten, Thomas B Schön, and Carl Edward Rasmussen. Bayesian Inference and Learning in Gaussian Process State-Space Models with Particle MCMC. *Advances in Neural Information Processing Systems*, 26, 2013.
- [13] Azad Ghaffari. Analytical Design and Experimental Verification of Geofencing Control for Aerial Applications. *IEEE/ASME Transactions on Mechatronics*, 26:1106–1117, 2021.

- [14] Paul Griffioen, Alex Devonport, and Murat Arcak. Probabilistic Invariance for Gaussian Process State Space Models. In *Learning for Dynamics and Control Conference*, pages 458–468. PMLR, 2023.
- [15] Lukas Hewing, Andrea Carron, Kim P Wabersich, and Melanie N Zeilinger. On a Correspondence Between Probabilistic and Robust Invariant Sets for Linear Systems. In *2018 European Control Conference (ECC)*, pages 1642–1647. IEEE, 2018.
- [16] Maryam Kamgarpour, Jerry Ding, Sean Summers, Alessandro Abate, John Lygeros, and Claire Tomlin. Discrete Time Stochastic Hybrid Dynamical Games: Verification & Controller Synthesis. In *2011 50th IEEE Conference on Decision and Control and European Control Conference*, pages 6122–6127. IEEE, 2011.
- [17] Ernesto Kofman, José A De Doná, and Maria M Seron. Probabilistic Set Invariance and Ultimate Boundedness. *Automatica*, 48(10):2670–2676, 2012.
- [18] Ernesto Kofman, José A De Doná, Maria M Seron, and Noelia Pizzi. Continuous-Time Probabilistic Ultimate Bounds and Invariant Sets: Computation and Assignment. *Automatica*, 71:98–105, 2016.
- [19] Johan Lofberg. YALMIP: A Toolbox for Modeling and Optimization in MATLAB. In *2004 IEEE International Conference on Robotics and Automation*, pages 284–289. IEEE, 2004.
- [20] MOSEK ApS. *The MOSEK Optimization Toolbox for MATLAB Manual. Version 9.3.6*, 2019.
- [21] Sampath Kumar Mulagaleti, Alberto Bemporad, and Mario Zanon. Data-Driven Synthesis of Robust Invariant Sets and Controllers. *IEEE Control Systems Letters*, 6:1676–1681, 2021.
- [22] Noelia Pizzi, Ernesto Kofman, Damián Edgardo Marelli, José Adrian De Doná, and Maria M Seron. Probabilistic ultimate bounds and invariant sets in nonlinear systems. *Automatica*, 133:109853, 2021.
- [23] Carl Edward Rasmussen and Christopher KI Williams. *Gaussian Processes for Machine Learning*, volume 2. MIT Press Cambridge, MA, 2006.
- [24] Jeff Schneider. Exploiting Model Uncertainty Estimates for Safe Dynamic Control Learning. *Advances in Neural Information Processing Systems*, 9, 1996.
- [25] Alberto Seeger. Direct and Inverse Addition in Convex Analysis and Applications. *Journal of Mathematical Analysis and Applications*, 148(2):317–349, 1990.
- [26] Danbing Seto and Lui Sha. *An Engineering Method for Safety Region Development*. Citeseer, 1999.
- [27] Andreas Svensson, Arno Solin, Simo Särkkä, and Thomas Schön. Computationally Efficient Bayesian Learning of Gaussian Process State Space Models. In *Artificial Intelligence and Statistics*, pages 213–221. PMLR, 2016.
- [28] Andrew Taylor, Andrew Singletary, Yisong Yue, and Aaron Ames. Learning for Safety-Critical Control with Control Barrier Functions. In *Learning for Dynamics and Control*, pages 708–717. PMLR, 2020.
- [29] Ryan Turner, Marc Deisenroth, and Carl Rasmussen. State-Space Inference and Learning with Gaussian Processes. In *Proceedings of the Thirteenth International Conference on Artificial Intelligence and Statistics*, pages 868–875. JMLR Workshop and Conference Proceedings, 2010.
- [30] Jonas Umlauft and Sandra Hirche. Learning Stochastically Stable Gaussian Process State-Space Models. *IFAC Journal of Systems and Control*, 12:100079, 2020.
- [31] Li Wang, Evangelos A Theodorou, and Magnus Egerstedt. Safe Learning of Quadrotor Dynamics Using Barrier Certificates. In *2018 IEEE International Conference on Robotics and Automation (ICRA)*, pages 2460–2465. IEEE, 2018.
- [32] Ang Xie, Feng Yin, Bo Ai, Sha Zhang, and Shuguang Cui. Learning While Tracking: A Practical System Based on Variational Gaussian Process State-Space Model and Smartphone Sensory Data. In *2020 IEEE 23rd International Conference on Information Fusion (FUSION)*, pages 1–7. IEEE, 2020.
- [33] Aijun Yin, Junlin Zhou, and Tianyou Liang. A Gaussian Process State Space Model Fusion Physical Model and Residual Analysis for Fatigue Evaluation. *Sensors*, 22(7):2540, 2022.
- [34] Yan Zeng, Jiantao Yang, and Yuehong Yin. Gaussian Process-Integrated State Space Model for Continuous Joint Angle Prediction from EMG and Interactive Force in a Human-Exoskeleton System. *Applied Sciences*, 9(8):1711, 2019.
- [35] Fuzhen Zhang. *The Schur Complement and Its Applications*, volume 4. Springer Science & Business Media, 2006.
- [36] Bingzhuo Zhong, Abolfazl Lavaei, Majid Zamani, and Marco Caccamo. Automata-Based Controller Synthesis for Stochastic Systems: A Game Framework via Approximate Probabilistic Relations. *Automatica*, 147:110696, 2023.
- [37] Bingzhuo Zhong, Majid Zamani, and Marco Caccamo. Synthesizing Safety Controllers for Uncertain Linear Systems: A Direct Data-Driven Approach. In *2022 IEEE Conference on Control Technology and Applications (CCTA)*, pages 1278–1284. IEEE, 2022.



Paul Griffioen is currently a post-doctoral researcher in the Department of Electrical Engineering and Computer Sciences at the University of California, Berkeley working with Murat Arcaç. He received the B.S. degree in Electrical and Computer Engineering from Calvin College, Grand Rapids, MI, USA in 2016 and the

M.S. and Ph.D. degrees in Electrical and Computer Engineering from Carnegie Mellon University, Pittsburgh, PA, USA in 2018 and 2022, respectively. His research interests include the modeling, analysis, and design of high-performance cyber-physical systems that ensure safety while operating under computational constraints. His research interests also include the modeling, analysis, and design of active detection techniques and response mechanisms for ensuring resilient and secure cyber-physical systems.



Bingzhuo Zhong is an Assistant Professor in the Thrust of Artificial Intelligence, Information Hub, at the Hong Kong University of Science and Technology (Guangzhou), China. He received a Dr. rer. nat. degree in Computer Science (summa cum laude) in 2023 and an M.Sc. degree in Mechanical Engineering in 2018 from the Technical University of Munich, Germany,

and a B.Eng. degree in Vehicle Engineering in 2016 from Tongji University, China. In 2023, he was a visiting researcher at the University of California, Berkeley. Between October 2023 and July 2024, he was a postdoctoral researcher at the University of Colorado Boulder and the University of California, Berkeley, USA. His research interests include formal methods for trustworthy artificial intelligence, safety and security of Cyber-Physical Systems, and data-driven control.



Murat Arcaç is a professor at U.C. Berkeley in the Electrical Engineering and Computer Sciences Department, with a courtesy appointment in Mechanical Engineering. He received the B.S. degree in Electrical Engineering from the Bogazici University, Istanbul, Turkey (1996) and the M.S. and Ph.D. degrees from the University of California, Santa Barbara (1997 and 2000). His research is in dynamical systems and control theory with applications in multi-agent systems and transportation. He received a CAREER Award from the National Science Foundation in 2003, the Donald P. Eckman Award from the American Automatic Control Council in 2006, the Control and Systems Theory Prize from the Society for Industrial and Applied Mathematics (SIAM) in 2007, and the Antonio Ruberti Young Researcher Prize from the IEEE Control Systems Society in 2014. He is a mem-

ber of ACM and SIAM, and a fellow of IEEE and the International Federation of Automatic Control (IFAC).



Majid Zamani is an associate professor in the Computer Science Department at the University of Colorado Boulder. Between May 2014 and January 2019, he was an assistant professor in the Department of Electrical Engineering at Technical University of Munich where he led the Hybrid Control Systems Group. He received a Ph.D. degree in Electrical Engineering and an MA degree in Mathematics both from the University of California, Los Angeles in 2012, an M.Sc. degree in Electrical Engineering from Sharif University of Technology in 2007, and a B.Sc. degree in Electrical Engineering from Isfahan University of Technology in 2005. He received the George S. Axelby Outstanding Paper Award from the IEEE Control Systems Society in 2023, the NSF CAREER award in 2022 and ERC starting grant and ERC Proof of Concept grant from the European Research Council in 2018 and 2023, respectively. His research interests include verification and control of cyber-physical systems, secure-by-construction synthesis, and compositional analysis and synthesis of interconnected systems.

Marco Caccamo studied Computer Engineering at University of Pisa (Italy). Following his degree in computer engineering in July 1997, he earned his Ph.D. in computer engineering from Scuola Superiore Sant'Anna (Italy) in 2002. Shortly after graduation, he joined the University of Illinois at Urbana-Champaign as assistant professor in Computer Science and was promoted to full professor in 2014. Since 2018, he has been appointed to the chair of Cyber-Physical Systems in Production Engineering at the Technical University of Munich, Germany. Prof. Caccamo received visiting professorships at ETH, Zurich and TUM Munich as TÜV Süd Stiftung visiting professor and August-Wilhelm Scheer guest professor. He has chaired Real-Time Systems Symposium and Real-Time and Embedded Technology and Applications Symposium, the two IEEE flagship conferences on Real-Time Systems. He also served as General Chair of Cyber Physical Systems Week. In 2003, he was awarded an NSF CAREER Award. He is a recipient of the Alexander von Humboldt Professorship and he is an IEEE Fellow.



Science and was promoted to full professor in 2014. Since 2018, he has been appointed to the chair of Cyber-Physical Systems in Production Engineering at the Technical University of Munich, Germany. Prof. Caccamo received visiting professorships at ETH, Zurich and TUM Munich as TÜV Süd Stiftung visiting professor and August-Wilhelm Scheer guest professor. He has chaired Real-Time Systems Symposium and Real-Time and Embedded Technology and Applications Symposium, the two IEEE flagship conferences on Real-Time Systems. He also served as General Chair of Cyber Physical Systems Week. In 2003, he was awarded an NSF CAREER Award. He is a recipient of the Alexander von Humboldt Professorship and he is an IEEE Fellow.